Sudan University of Science and Technology
College of graduate

Numerical Study of Unsteady Boundary layer Flow over a Stretching Surface in Rotating Fluid

دراسة عددية لانسياب الطبقة الحدية غير المستقر علي سطح متمدد في مائع دوار

A THESIS SUBMITTED IN PARTIAL FULFILMENT OF THE DEGREE OF M. Sc. IN MATHEMATICS

By: Ekram Saeed Abass Saeed

Supervisor: Dr. Faiz G. A. Awad

November 2016

Contents

Abstract in Arabic

تمت دراسة الحركه غير المستقرة لمائع لزج غير قابل للانضغاط على سطح متمدد . باستخدام تقريبات الطبقه الحديه حولت معادلات العزم النصف قطري والدائري الى معادلات تفاضليه جزئيه عالية الخطيه بعد ذلك حلت عدديا بطريقة الطيف محلية الخطيه ومن ثم تم توضيح تاثيرات معامل التدوير على خصائص المائع في صورة رسومات وجداول.

Abstract

The two-dimensional an incompressible rotating viscous fluid flow over unsteady stretching surface is investigated. Using the boundary layer approximation, the two-dimensional axial and angular momentum equations are transferred into highly non-linear partial differential equations form and solved numerically using the spectral local linearisation method. The effects of rotating coefficient on the fluid properties are determined and shown graphically and in tabular form.

Dedication

To

my father . . .

my mother . . .

my brothers . . .

my sisters . . .

and my friends . . .

Acknowledgements

First of all, I am grateful to Allah for helping me to complete thesis. I would like to express my appreciation to Dr.Faiz for his guidance during the term of this course. Without his valuable assistance, this work would not have been completed. I would also like to thank Dr.Mohamed Abdelaziz and Dr.Mohamed Khabir for their support and cooperation. Special thanks to my friends who helped me. Finally, I would like to thank my parents, brothers and sisters for their unconditional love,support and encouragement.

Chapter 1

Introduction

The unsteady boundary layer flow over a moving surface has been an active area of investigation for along time due its wide range of applications in industrial processes such as the cooling of an infinite metallic plate in a cooling bath, the aerodynamic extrusion of plastic sheets, boundary layer along the material handling conveyers, the boundary layer along a liquid film and condensation processes. The quality of the final product depends on the skin friction coefficient and the rate of heat transfer. The most earliest studies in the unsteady boundary layer flow was curried out by Sakiadis [1, 2]. Later Cranke [3] studied the problem in two-dimensional for the elastic flat plate. Studies have been carried out for the case of the axisymmetric and three-dimensional flow by Brady and Acrivos [4], and Wang [5]. Investigations by, among others, Afzal [6], Prasad et al. [7], Abel and Mahesha [8], Abel et al. [9], Bataller [10], have also provided examples of various aspects of this important field.

Rotating effect on the unsteady flow and the surface included in many

applications such as chemical and geophysical fluid dynamics and mechanical nuclear engineering. The problem of unsteady rotating flow of incompressible, viscous fluid past an infinite porous plate was investigated by Soundalgekar [11] using the Fourier series. The boundary layer flow problem formed in a rotating fluid by oscillating flow over an infinite half-plate has been examined Bergstrom [12]. Abbas et al. [13] studied the unsteady boundary layer MHD flow and heat transfer on a stretching continuous sheet in a viscous incompressible rotating fluid numerically using the Keller-box method. Nazar et al. [14] investigated unsteady flow due to the impulsive starting from rest of a stretching surface in a viscous and incompressible rotating fluid. Zheng et al. [15] studied the unsteady rotating flow of a generalized Maxwell fluid with fractional derivative model between two infinite straight circular cylinders. Using the shooting method Fang [16] studied the problem of the laminar unsteady flow over a stretchable rotating disk with deceleration is investigated. Rashad [17] investigated the unsteady magnetohydrodynamics boundary-layer flow and heat transfer for a viscous laminar incompressible electrically conducting and rotating fluid due to a stretching surface embedded in a saturated porous medium with a temperature-dependent viscosity in the presence of a magnetic field and thermal radiation effects. Nageeb et al. [18] used the Runge-Kutta method based on shooting technique to investigate the unsteady MHD flow and heat transfer of a couple stress fluid over a rotating disk. For the case in which steady flow rotating flow involve the power-law, very recently, Hajmohammadi et al. [19] developed an analytical solution for two-phase flow betwen two rotating cylinders filed with power law liquid and a micro layer of gas. Moreover Hajmohammadi and Nourazar [20] the problem of heat transfer repercussions thin gas layer in micro cylindrical Couette flows involving power-law liquids.

Unsteady flows are mostly defined or modeled by systems of nonlinear PDEs which more difficult to solve than steady flows problems which are often simplified into system nonlinear ODEs using the so-called similarity transformations (see Motsa et al. [21]). Finding solutions of the PDEs governing the fluid model plays a crucial role in understanding the behavior of this model. Mostly, these PDEs are highly nonlinear and not easy to find exact solution, hence various analytical and numerical methods have been employed to approximate the solutions of these problems such as homotopy analysis method, spectral method, Keller box method, finite difference method, finite element and finite volume methods. Spectral methods are generally the most accurate through all these method for problems with smooth solutions. Based on spectral method Motsa et al. [22] established the so called spectral relaxation method (SRM) to solve nonlinear differential equations. The method has been used in the solution of PDEs by Motsa et al.[21] and ODEs for example the chaotic and hyper-chaotic systems [23, 24]. The SRM is based on simple decoupling and rearrangement of the governing nonlinear equations in a Gauss-Seidel manner. The resulting sequence of equations are integrated using the Chebyshev spectral collocation method.

The aim of this work is to investigate the problem of an unsteady flow over stretching surface in a rotating fluid, which has been introduced by Nazar et al. [25]

Chapter 2

Unsteady flow over stretching surface in a rotating fluid

Consider the two dimensional stretching of a surface in a rotating fluid. At time $t = 0$, the surface at $z = 0$ impulsively stretched in the x direction in a rotating fluid. Due to the Coriolis force, the fluid motion is three-dimensional. Let $(\mathrm{u}, \mathrm{v}, \mathrm{w})$ be the velocity components in the direction of the Cartesian axes (x, y, z), respectively, with the axes rotating at an angular velocity Ω in the z direction. The unsteady Navier-Stokes equations governing the flow are

$$\frac{\partial \mathrm{u}}{\partial x} + \frac{\partial \mathrm{v}}{\partial y} + \frac{\partial \mathrm{w}}{\partial z} = 0, \tag{2.1}$$

$$\frac{\partial \mathrm{u}}{\partial t} + \mathrm{u}\frac{\partial \mathrm{u}}{\partial x} + \mathrm{v}\frac{\partial \mathrm{u}}{\partial y} + \mathrm{w}\frac{\partial u}{\partial z} - 2\Omega \mathrm{v} = -\frac{1}{\rho}\frac{\partial p}{\partial x} + \nu \nabla^2 \mathrm{u}, \tag{2.2}$$

$$\frac{\partial \mathrm{v}}{\partial t} + \mathrm{u}\frac{\partial \mathrm{v}}{\partial x} + \mathrm{v}\frac{\partial \mathrm{v}}{\partial y} + \mathrm{w}\frac{\partial v}{\partial z} - 2\Omega \mathrm{u} = -\frac{1}{\rho}\frac{\partial p}{\partial y} + \nu \nabla^2 \mathrm{v}, \tag{2.3}$$

$$\frac{\partial \mathrm{w}}{\partial t} + \mathrm{u}\frac{\partial \mathrm{w}}{\partial x} + \nu\frac{\partial \mathrm{w}}{\partial y} + \mathrm{w}\frac{\partial \mathrm{w}}{\partial z} = -\frac{1}{\rho}\frac{\partial p}{\partial z} + \nu \nabla^2 \mathrm{w}, \tag{2.4}$$

where p is the pressure, ρ is the density, ν is the kinematic viscosity and ∇^2 denotes the three-dimensional Laplacian. Let the surface be impulsively stretched in the x direction such that the initial and boundary condition

$$\begin{aligned} &t < 0 : \mathrm{u} \;=\; \mathrm{v} \;=\; \mathrm{w} \;=\; 0 \;\; \text{for} \;\; \text{any} \;\; x, y, z, \\ &t \geq 0 : \mathrm{u} = ax, \;\; \mathrm{v} = 0, \;\; \mathrm{w} = 0 \quad \text{at} \;\; z = 0, \\ &\mathrm{u} \longrightarrow 0, \mathrm{v} \longrightarrow 0, \mathrm{w} \longrightarrow 0 \;\; \text{at} \;\; z \longrightarrow \infty, \end{aligned} \tag{2.5}$$

where $a > 0$ has the dimension of $[t^{-1}]$ and represents the stretching rate. We now introduce the following similarity variables

$$\begin{aligned} &\eta = (a/\nu)^{1/2}\xi^{-1/2}z, \;\; \mathrm{u} = axf'(\xi,\eta), \;\; \mathrm{v} = axh(\xi,\eta), \\ &\mathrm{w} = -(a\nu)^{1/2}\xi^{1/2}f(\xi,\eta), \;\; \xi = 1 - \exp^{-\tau}, \;\; \tau = at. \end{aligned} \tag{2.6}$$

Substituting Eqn(2.6) into the governing equations (2.2)-(2.4), yield to

$$f''' + \frac{1}{2}(1-\xi)\eta f'' + \xi(ff'' - f'^2 + 2\lambda h) = \xi(1-\xi)\frac{\partial f'}{\partial \xi}, \tag{2.7}$$

$$h'' + \frac{1}{2}(1-\xi)\eta h' + \xi(fh' - f'h - 2\lambda f') = \xi(1-\xi)\frac{\partial h}{\partial \xi}, \tag{2.8}$$

subject to the boundary conditions

$$f(\xi,0) = 0, \;\; f'(\xi,0) = 1, \;\; h(\xi,0) = 0, \;\; f'(\xi,\infty) = 0, \;\; h(\xi,\infty) = 0, \tag{2.9}$$

where $\lambda = \Omega/a$.

The non-dimensional skin friction in both the x and y directions are

defined in the form

$$C_f^x = \frac{\tau_w^x}{\rho(ax)^2}\ , \quad C_f^y = \frac{\tau_w^y}{\rho(ax)^2}, \tag{2.10}$$

where, the wall shear stresses τ_w^x, τ_w^y, respectively, are given by

$$\tau_w^x = \mu\left(\frac{\partial \mathrm{u}}{\partial z}\right)_{z=0}, \quad \tau_w^y = \mu\left(\frac{\partial \mathrm{v}}{\partial z}\right)_{z=0}. \tag{2.11}$$

By substituting (2.11) into Eqn (2.10), we obtain

$$C_f^x Re_x^{1/2} = \xi^{-1/2} f''(\xi, 0), \quad C_f^y Re_x^{1/2} = \xi^{-1/2} h'(\xi, 0), \tag{2.12}$$

where $Re_x = (ax)x/\nu$ is the local Reynolds number.

2.1 Initial solution at $\xi = 0$

For $\xi = 0$ (initial unsteady flow), corresponding to $\tau = 0$, Eqn.(2.7) can be written in the form

$$f''' + \frac{1}{2}\eta f'' = 0, \tag{2.13}$$

subject to the boundary conditions

$$f(0,0) = 0, \quad f'(0,0) = 1, \quad f'(0,\infty) = 0. \tag{2.14}$$

Hence, solution of this equation takes the form

$$f(\eta) = \eta \mathrm{erfc}(\eta/2) + \frac{2}{\sqrt{\pi}}(1 - e^{-\eta^2/4}), \tag{2.15}$$

with $f'(\eta) = \text{erfc}(\eta/2)$, where $\text{erfc}(\eta/2)$ is the complementary error function defined as

$$\text{erfc}(\eta/2) = \frac{2}{\sqrt{\pi}} \int_{\frac{\eta}{2}}^{\infty} e^{-s^2} ds, \tag{2.16}$$

Chapter 3

The Spectral Local Linearisation

3.1 General governing equation system

Consider a system of m nonlinear ordinary differential equations in m unknowns functions $z_i(\eta)$ $i = 1, 2, 3, ..., m$ where η is the independent variable. The system can be written as a sum of it's linear $\mathbf{L}$ and nonlinear components $\mathbf{N}$ as

$$\mathbf{L}\left[z_1\left(\eta\right), z_2\left(\eta\right), ..., z_m\left(\eta\right)\right] + \mathbf{N}\left[z_1(\eta), z_2\left(\eta\right), ..., z_m(\eta)\right] = \mathbf{H}\left(\eta\right), \quad (\eta) \in (a, b), \tag{3.1}$$

subject to the boundary conditions

$$A_i\left[z_1\left(a\right), z_1\left(a\right), ..., z_m\left(a\right)\right] = K_{a,i}, \quad B_i\left[z_1\left(b\right), z_2\left(b\right), ..., z_m(b)\right] = K_{b,i}, \tag{3.2}$$

where A_i and B_i are linear operators and $K_{a,i}$ and $K_{b,i}$ are constants for $i = 1, 2, ..., m$. Define the vector Z_i to be the vector of the derivatives

of the variable z_i with respect to the dependent variable η, that is

$$Z_i = \left[z_i^{(0)}, z_i^{(1)}, ..., z_i^{(n_i)} \right], \tag{3.3}$$

where $z_i^{(0)} = z_i$, $z_i^{(p)}$ is the p^{th} derivative of z_i with respect to η and $n_i \, (i = 1, 2, .., m)$ is the highest derivative order of the variable z_i appearing in the system of equations. In addition, we define $\mathbf{L}_i$ and $\mathbf{N}_i$ to be the linear and nonlinear operators, respectively, that operate on the Z_i for $i = 1, 2, .., m$, with these definitions,equation (3.1) and (3.2) can be written as

$$\mathbf{L}_i \left[Z_1, Z_2, ...Z_m \right] + \mathbf{N}_i \left[Z_1, Z_2, ...Z_m \right] = \sum_{j=1}^{m} \sum_{p=0}^{n_i} \alpha_{i,j}^{[p]} z_j^{(p)} + \mathbf{N}_i \left[Z_1, Z_2, ...Z_m \right] = \mathbf{H}_i, \tag{3.4}$$

where $\alpha_{i,j}^{[p]}$ are the constant coefficient of $z_j^{(p)}$, the derivative of $z_j \, (j = 1, 2, ...m)$ that appears in the i^{th} equation for $i = 1, 2, ..., m$. Noting that, for each variable z_i in the derivatives in the boundary conditions can at most be one less than the highest derivative of z_i in the governing system (3.1) we define the vector $\tilde{\mathbf{Z}}_i$ to be the vector of the derivatives of the variable z_i with respect to the dependent variable η from 0 up to $(n_i - 1)$, that is

$$\tilde{\mathbf{Z}}_i = \left[z_i^{(0)}, z_i^{(1)}, ..., z_i^{(n_i - 1)} \right], \tag{3.5}$$

The boundary conditions(3.2) can be written as

$$A_\nu \left[\tilde{\mathbf{Z}}_1(a), \tilde{\mathbf{Z}}_2(a), ..., \tilde{\mathbf{Z}}_m(a) \right] = \sum_{j=1}^{m} \sum_{p=0}^{n_j - 1} \beta_{\nu,j}^{[p]} z_j^{(p)} \, (a) = K_{a,\nu}, \nu = 1, 2, ..., m_a, \tag{3.6}$$

$$B_\sigma \left[\tilde{\mathbf{Z}}_1(b), \tilde{\mathbf{Z}}_2(b), ..., \tilde{\mathbf{Z}}_m(b)\right] = \sum_{j=1}^{m} \sum_{p=0}^{n_j-1} \gamma_{\sigma,j}^{[p]} z_j^{(p)}(b) = K_{b,\sigma}, \sigma = 1, 2, ..., m_b, \tag{3.7}$$

where $\beta_{\nu,j}^{[p]}$ and $\gamma_{\sigma,j}^{[p]}$ are the constant coefficients of $z_j^{(p)}$ in the boundary conditions, and m_a, m_b, are the total number of prescribed boundary condition, at $x = a$ and $x = b$ respectively. We remark that the sum $m_a + m_b$ is equal to the sum of the highest orders of the derivatives corresponding to the dependent variable z_i,that is

$$m_a + m_b = \sum_{i=1}^{m} n_i, \tag{3.8}$$

3.2 Spectral Local linearisation Method (SLLM)

Let us consider a system of m nonlinear ordinary differential equations in m unknowns functions $z_i(\eta)$ $i = 1, 2, 3, ..., m$ where η is the independent variable. The system can be written as a sum of it's linear $\mathbf{L}$ and nonlinear components $\mathbf{N}$ as

$$\mathbf{L}\left[z_1(\eta), z_2(\eta), ..., z_m(\eta)\right] + \mathbf{N}\left[z_1(\eta), z_2(\eta), ..., z_m(\eta)\right] = \mathbf{H}(\eta), \quad \eta \in [a, b], \tag{3.9}$$

To develop the iteration scheme, we apply local linearisation of N_i about $Z_{i,r}$ (the previous iteration) to the i^{th} non-linear equation assuming that all other $Z_{k,r}(k \neq i)$ are known. Thus, at the ith equation, N_i is linearised as follows

$$Ni[Z_1, Z_2, ..., Z_m] = N_i[Z_{1,r}, ..., Z_{m,r}] + \frac{\partial N_i}{\partial Z_i}[Z_{1,r}, Z_{2,r}, ..., Z_{m,r}](Z_{i,r+1} - Z_{i,r}), \tag{3.10}$$

$$L_i[Z_{1,r+1}, ..., Z_{m,r+1}] + \frac{\partial N_i}{\partial Z_i}[...]Z_{i,r+1} = H_i + \frac{\partial N_i}{\partial Z_i}[...]Z_{i,r} - Ni[Z_{1,r}, ..., Z_{m,r}], \tag{3.11}$$

where [...] denotes $[Z_{1,r}, Z_{2,r}, ..., Z_{m,r}]$ and $Z_{i,r+1}$ and $Z_{i,r}$ are the approximations of Z_i at the current and the previous iteration, respectively. Thus, starting from an initial approximation $Z_{1,0}, Z_{2,0}, ..., Z_{m,0}$, the proposed iterative scheme (3.9) is then solved as a loop until the system converges at a consistent solution for all the variables. To solve the iteration scheme (3.9), it is convenient to use the Chebyshev pseudo-spectral method as in previous section. For this reason the proposed method is referred to as the spectral local linearization iteration method (SLLM). Before applying the spectral method, it is convenient to transform the domain on which the governing equation is defined to the interval $[-1, 1]$ on which the spectral method can be implemented. We use the transformation $\eta = (b-a)(t+1)/2$ to map the interval $[a, b]$ to $[-1, 1]$. The basic idea behind the spectral collocation method is the introduction of a differentiation matrix $\mathbf{D}$ which is used to approximate the derivatives of the unknown variables $z_i(\eta)$ at the collocation points as the matrix vector product

$$\frac{dZ_i}{d\eta} = \sum_{j=1}^{m} \sum_{k=0}^{\widehat{N}} \mathbf{D}_{lk} Z_i(t_k) = DZ_i, \quad l = 0, 1, ..., \widehat{N} \tag{3.12}$$

where $\widehat{N} + 1$ is the number of collocation points (grid points), $\mathbf{D} = 2D/(b-a)$, and $Z = [z(t_0), z(t_1), ..., z(t_N)]^T$ is the vector function at the collocation points. Higher order derivatives are obtained as powers of $\mathbf{D}$, that is

$$Z_j^{(p)} = D_p Z_j. \tag{3.13}$$

Chapter 4

Numerical Solution

In this part we present the numerical method used to solve the governing nonlinear system of PDEs $(2.7)-(2.8)$ along with boundary conditions (2.9). For the implementation of the spectral collocation method, at a later stage, it is convenient to reduce the order of equation (2.7) from three to two. To this end, we set $f' = u$, so that equation (2.7) becomes

$$u'' + \frac{1}{2}\eta(1-\xi)u' + \xi(fu' - u^2 + 2\lambda h) = \xi(1-\xi)\frac{\partial u}{\partial \xi}, \quad (4.1)$$

$$f' = u. \quad (4.2)$$

The spectral local linearisation method(SLLM) approach is used to decouple the equations leading to a linear system which is subsequently solved using the Chebyshev spectral collocation method. The basic idea behind the SLLM stems from the combination of the Gauss-Seidel method for decoupling equations and the Newton-Raphson based quasi-

linearisation. In this regard, linearisation in the momentum equation (4.1) is applied only in terms involving $u(\eta)$ and its derivatives. All other terms are assumed to be known from previous iterations. The terms involving $h(\eta)$ are assumed to be known from previous iteration while the updated solution for $u(\eta)$ at the current iteration is used. Similarly, in Eqn (2.8), only terms in $h(\eta)$ are linearised while terms in $u(\eta)$ are assumed to be now known at the current iteration (denoted by $(r+1)$). Thus applying the LLM on Eqns (2.9), (4.1) and (4.2) gives

$$u''_{r+1} + a_{1,r}u'_{r+1} + a_{2,r}u_{r+1} = a_{3,r} + \xi(1-\xi)\frac{\partial u_{r+1}}{\partial \xi}, \tag{4.3}$$

$$f'_{r+1} = u_r, \tag{4.4}$$

$$h''_{r+1} + b_{1,r}h'_{r+1} + b_{2,r}h_{r+1} = b_{3,r} + \xi(1-\xi)\frac{\partial h_{r+1}}{\partial \xi}, \tag{4.5}$$

where the primes denote partial derivatives with respect to η. The boundary conditions are given by

$$\begin{aligned} &f_{r+1}(\eta,0) = 0, \quad u_{r+1}(\eta,0) = 1, \quad h_{r+1}(\eta,0) = 0, \\ &u_{r+1}(\eta,\infty) = 0, \quad h_{r+1}(\eta,\infty) = 0. \end{aligned} \tag{4.6}$$

The coefficients in (4.4) and (4.5) are defined as

$$\begin{aligned} a_{1,r} &= \frac{1}{2}(1-\xi)\eta + \xi f_r, \qquad a_{2,r} = -2\xi u_r, \\ a_{3,r} &= -\xi u_r^2 - 2\lambda\xi h_r, \\ b_{1,r} &= \frac{1}{2}(1-\xi)\eta + \xi f_r, \quad b_{2,r} = -\xi u_r, \quad b_{3,r} = 2\lambda\xi u_r. \end{aligned} \tag{4.7}$$

To solve the linearised system of $(4.3)-(4.5)$ we employ the Chebyshev spectral collocation method to discretize in the η- direction and use an implicit finite difference method in the ξ-direction. To this end, we

define the grid points on (η, ξ) as

$$\eta_j = \cos\frac{\pi_j}{N_\eta}, \quad \xi^n = n\Delta\xi, \tag{4.8}$$
$$j = 0, 1, ..., N_\eta; n = 0, 1, ..., N_\xi,$$

where N_η, N_ξ are the total number of grid points in the η- and ξ-direction, respectively, and $\Delta\xi$ is the spacing in the ξ-direction. The finite difference scheme is applied with centering about a midpoint halfway between ξ^{n+1} and ξ^n. This midpoint is defined as $\xi^{n+\frac{1}{2}} = (\xi^{n+1} + \xi^n)/2$. The derivatives with respect with η are discretized in terms of the Chebyshev differentiation matrices. Applying the centering about $\xi^{n+\frac{1}{2}}$ to any function, say $f(\eta, \xi)$ and its associated derivative, we obtain

$$f(\eta_j, \xi^{n+1/2}) = f_j^{n+1/2} = \frac{f_j^{n+1} + f_j^n}{2}, \tag{4.9}$$
$$\left(\frac{\partial f}{\partial \xi}\right)^{n+1/2} = \frac{f_j^{n+1} - f_j^n}{\Delta\xi}.$$

In applying the Chebyshev spectral collocation method, the continuous derivatives in the unknown functions are approximated by matrix-vector products of the so-called differentiation matrices at the collocation points. Before the spectral method is applied, the domain $\eta \in [0, \eta_\infty]$ is transformed to the domain $Y \in [-1, 1]$ by using the mapping $\eta = \eta_\infty(Y + 1)/2$. The basic idea behind the spectral collocation method is the introduction of a differentiation matrix D which is used to approximate the derivatives of the unknown variables f, u and h, at

the collocation points Y_j $(j = 0, 1, ..., N_\eta)$.

$$\left.\frac{\partial f}{\partial \eta}\right|_{\eta=\eta_j} = \sum_{k=0}^{N_\eta} D_{jk} f(Y_k, \xi) = \mathbf{D}F, \quad j = 0, 1, ..., N_\eta, \tag{4.10}$$

where $N_\eta + 1$ is the number of collocation points, $\mathbf{D} = 2D/\eta_\infty$, where the matrix D is of size $(N_\eta + 1)(N_\eta + 1)$ and its entries are defined as

$$\begin{aligned}
D_{jk} &= \frac{c_j(-1)^{j+k}}{c_k(Y_j - Y_k)}, \quad j \neq k;\ j, k = 0, 1, 2, 3, ..., N_\eta, \\
D_{kk} &= -\frac{Y_k}{2(1 - Y_k^2)}, \quad k = 1, 2, 3, ..., N_\eta - 1, \\
D_{00} &= \frac{2N_\eta^2 + 1}{6} = -D_{N_\eta N_\eta},
\end{aligned}$$

with

$$c_k = \begin{cases} 2, & k = 0, N_\eta; \\ 1, & -1 \leq k \leq N_\eta - 1. \end{cases} \tag{4.11}$$

which

$$\begin{aligned}
F &= [f(Y_0, \xi), f(Y_1, \xi), ..., f(Y_{N_\eta}, \xi)]^T, \\
U &= [u(Y_0, \xi), u(Y_1, \xi), ..., u(Y_{N_\eta}, \xi)]^T, \\
H &= [h(Y_0, \xi), h(Y_1, \xi), ..., h(Y_{N_\eta}, \xi)]^T,
\end{aligned}$$

are the vector functions at the collocation points. In general, a derivative of orders for the function $f(\eta)$ can be transformed as

$$f^{(s)}(\eta) \longrightarrow \mathbf{D}^{\mathbf{s}}F, \quad u^{(s)}(\eta) \longrightarrow \mathbf{D}^{\mathbf{s}}U, \quad h^{(s)}(\eta) \longrightarrow \mathbf{D}^{\mathbf{s}}H, \tag{4.12}$$

where s is the order of the derivative. Thus, applying the spectral local linearisation method in η and finite difference method in ξ gives

$$\begin{aligned} A_1 U_{r+1}^{n+1} &= B_1 U_{r+1}^{n} + K_1, \\ A_2 F_{r+1} &= K_2, \\ A_3 H_{r+1}^{n+1} &= B_3 H_{r+1}^{n} + K_3, \end{aligned} \tag{4.13}$$

where

$$\begin{aligned} A_1 &= \frac{1}{2}\left(\mathbf{D^2} + \mathbf{diag}[a_{1,r}]\mathbf{D} + \mathbf{diag}[a_{2,r}]\mathbf{I}\right) - \frac{\xi(1-\xi)}{\triangle\xi} \\ B_1 &= -\frac{1}{2}\left(\mathbf{D^2} + \mathbf{diag}[a_{1,r}]\mathbf{D} + \mathbf{diag}[a_{2,r}]\mathbf{I}\right) - \frac{\xi(1-\xi)}{\triangle\xi} \\ K_1 &= a_{1,r} \\ A_2 &= \mathbf{D}, \quad K_2 = u_r \\ A_3 &= \frac{1}{2}\left(\mathbf{D^2} + \mathbf{diag}[b_{1,r}]\mathbf{D} + \mathbf{diag}[b_{2,r}]\mathbf{I}\right) - \frac{\xi(1-\xi)}{\triangle\xi} \\ B_3 &= -\frac{1}{2}\left(\mathbf{D^2} + \mathbf{diag}[b_{1,r}]\mathbf{D} + \mathbf{diag}[b_{2,r}]\mathbf{I}\right) - \frac{\xi(1-\xi)}{\triangle\xi} \\ K_3 &= a_{1,r} \end{aligned}$$

with boundary conditions

$$\begin{aligned} &u_{r+1}(\eta_0, \xi^n) = 0, \ u_{r+1}(\eta_{N_e ta}, \xi^n) = 1, \\ &f_{r+1}(\eta_{N_\eta}, \xi^n) = 0, \\ &h_{r+1}(\eta_0, \xi^n) = 0, \ h_{r+1}(\eta_{N_\eta}, \xi^n) = 0, \end{aligned}$$

In the above equations H, U and F correspond to the approximate values of $h(\eta, \xi)$, $u(\eta, \xi)$ and $f(\eta, \xi)$ at the collocation points. The approximate solutions for f and h are obtained by solving (4.13). The convergence and stability of the iteration schemes are assessed by con-

sidering the norm of the difference in the values of the approximate functions between two successive iterations. Thus, for each iteration scheme, we define the following maximum error E at the $(r+1)th$ iteration:

$$E = \max(\|F_{r+1} - F_r\|_\infty, \|H_{r+1} - H_r\|_\infty). \tag{4.14}$$

The unknowns f and h were iteratively calculated, for a given number of collocation points N_η, until the following criteria for convergence was satisfied at iteration r :

$$E \leq \epsilon, \tag{4.15}$$

where ϵ is the convergence tolerance level.

Chapter 5

Results and Discussion

In this part we present the SLLM results for the solution of the governing equations(2.7) – (2.8). Numerical simulations were carried out to obtain approximate numerical values of the quantities of physical interest. In all the spectral method based numerical simulations a finite computational domain of extent $\eta_\infty = 20$ was chosen in the $\eta-$direction with $N_\eta = 60$. Through numerical experimentation, the computation of the value of any unknown, say F_{r+1}^{n+1}, at each time step is achieved by iterating using the local linearization method using a known value at the previous time step n as initial approximation. The iteration calculations are carried until some desired tolerance level, ϵ, is attained. In this study, the tolerance level was set to be $\epsilon = 10^{-8}$. The tolerance level is defined as the maximum values of the infinity norm of the difference between the values of the calculated quantities and its first two derivatives at successive iterations. For example, in calculating F_{r+1}^{n+1}, the tolerance level and convergence criteria is defined as

$$\max\{\|F_{r+1}^{n+1} - F_r^{n+1}\|_\infty,\ \|U_{r+1}^{n+1} - U_r^{n+1}\|_\infty,\ \|H_{r+1}^{n+1} - H_r^{n+1}\|_\infty\} < \epsilon. \quad (5.1)$$

Table 5.1: Values of $-f''(0,\xi)$ and $-h'(0,\xi)$ at different values of time ξ and λ

λ	ξ	$f''(0,\xi)$	$h'(0,\xi)$
	0.1	0.599346	0.331116
	0.3	0.598355	0.976621
1	0.5	0.500012	1.604727
	0.7	0.304455	2.229005
	0.9	0.013901	2.864634
	0.1	0.334264	1.673600
	0.3	-1.683855	5.409250
5	0.5	-5.090392	10.176826
	0.7	-9.269168	15.887446
	0.9	-14.042088	22.458498
	0.1	0.072655	2.367761
	0.3	-3.692311	8.148140
7	0.5	-9.522775	15.873009
	0.7	-16.631247	25.193909
	0.9	-24.688053	35.974353
	0.1	-0.472176	3.455217
	0.3	-7.419078	12.912358
10	0.5	-17.651836	25.815203
	0.7	-30.001110	41.553782
	0.9	-43.935681	59.843950

To obtain clear insights into the unsteadiness λ effects on the physics of

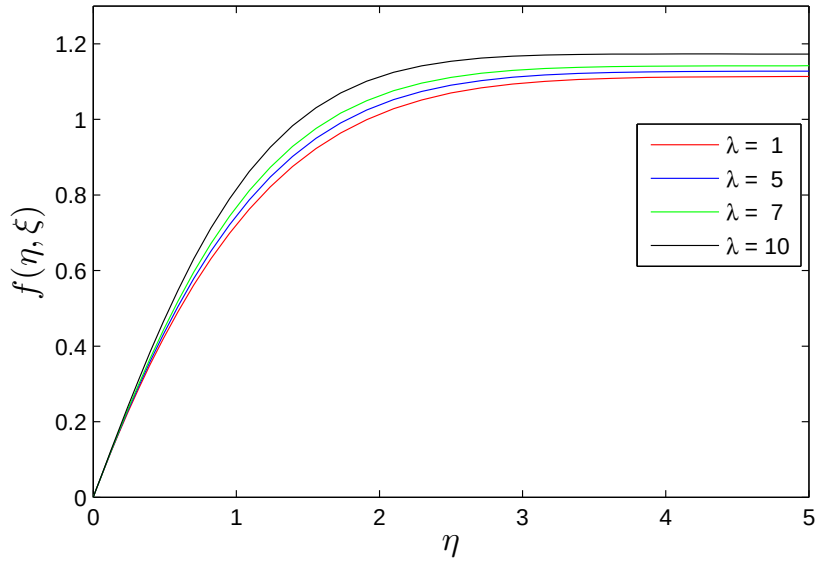

Figure 5.1: velocity profile in ξ direction for different value of λ

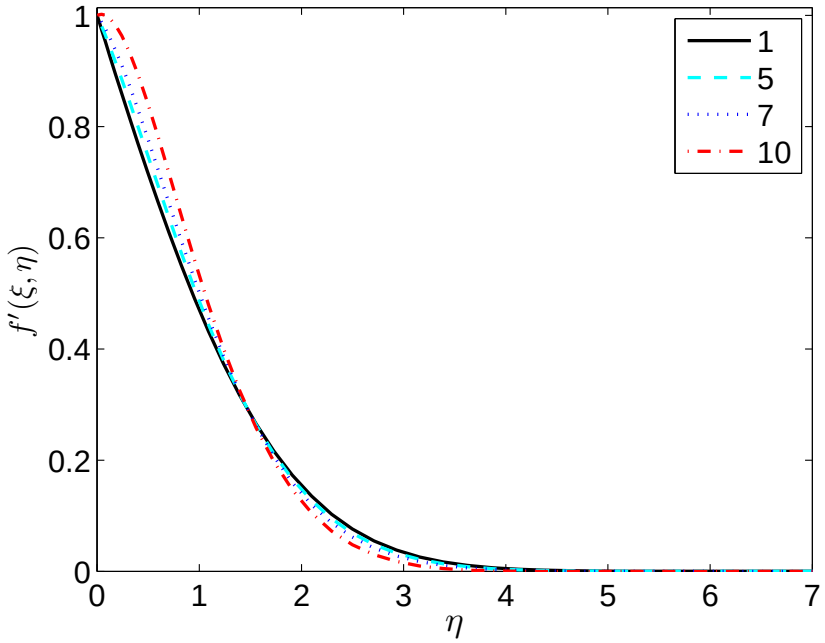

Figure 5.2: Velocity profiles for different values of λ

the problem, our approximate results for the axial velocity, angular ve-

locity and skin friction are presented graphically and in tabular forms. Table. The influence of λ on the fluid properties is give in Table 5.1 and Fig. 5.1 - 5.8.

Table. 5.1 gives the approximate numerical values of both the skin friction $f''(0,\xi)$ and $h'(0,\xi)$ for various values of λ. It is evident that as λ increases, the axial momentum boundary layer thickness decreases followed by a reduction in $f''(0,\xi)$, while the opposite behavior obtained in the case of $h'(0,\xi)$.

Fig. 5.1 and Fig. 5.2 show the variation of the axial velocity components $f(\eta,\xi)$ and $f'(\eta,\xi)$, respectively, for different values of λ. We observe that an increase in the values of λ leads to monotonic decrease in $f(\eta,\xi)$, while $f'(\eta,\xi)$ an increase in λ causing increasing in $f'(\eta,\xi)$ up to a certain critical point and then an exponential decay in the velocity profile obtained.

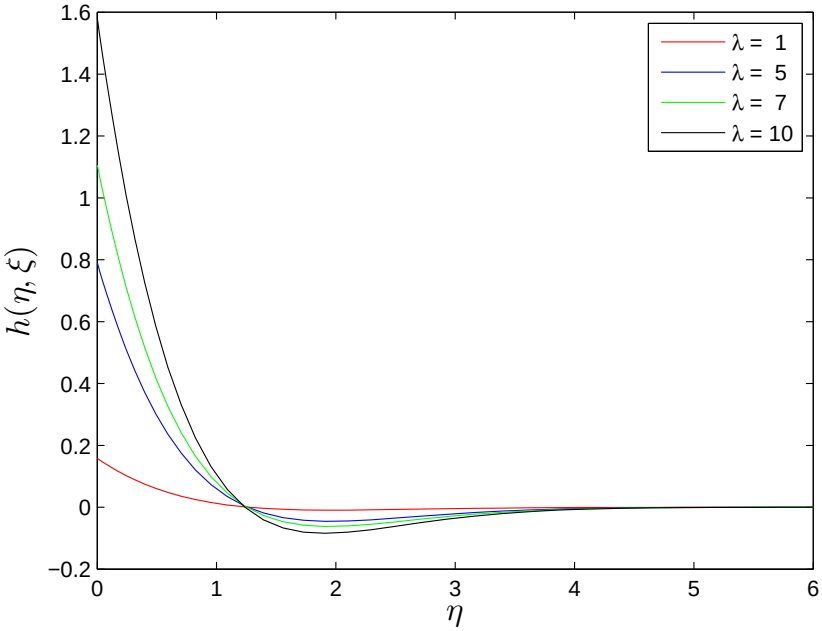

Figure 5.3: Velocity profiles for different values of λ

Fig. 5.3 illustrates the effects of λ on the angular velocity of the fluid

$h(\eta, \xi)$. We observe that $h(\eta, \xi)$ increases as λ increases.
Fig. 5.4 and Fig. 5.5 depict the variation of the skin friction coefficients $f''(0, \xi)$ and $-h'(0, \xi)$ respectively for different values of the λ. It is evident that as λ increases, the boundary layer thickness increases, then increase $f''(0, \xi)$ and $-h'(0, \xi)$. The axial and angular velocities vari-

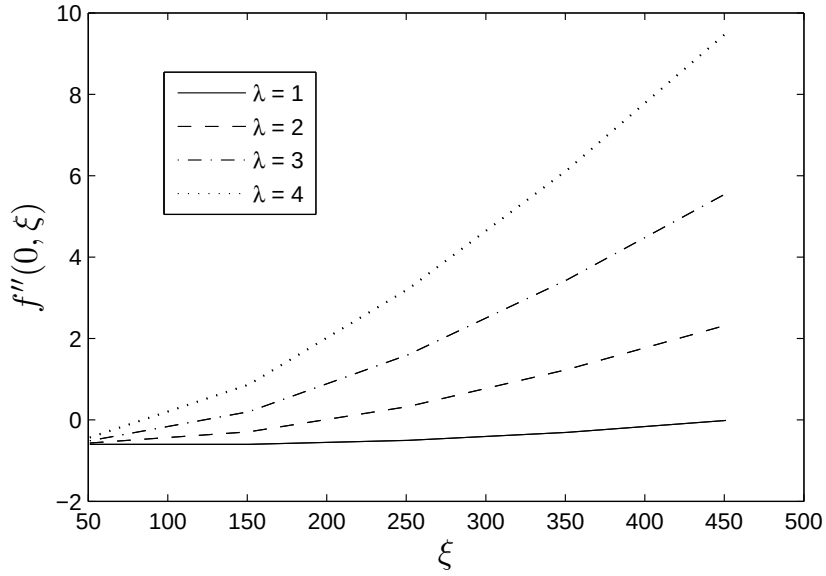

Figure 5.4: Skin friction variation for different values of λ

ation for different values of ξ are shown in Figs .5.6 - 5.8 respectively. From these figures, we observed that the transition from the initial unsteady state flow to the final steady state flow takes place smoothly and without any singularity.

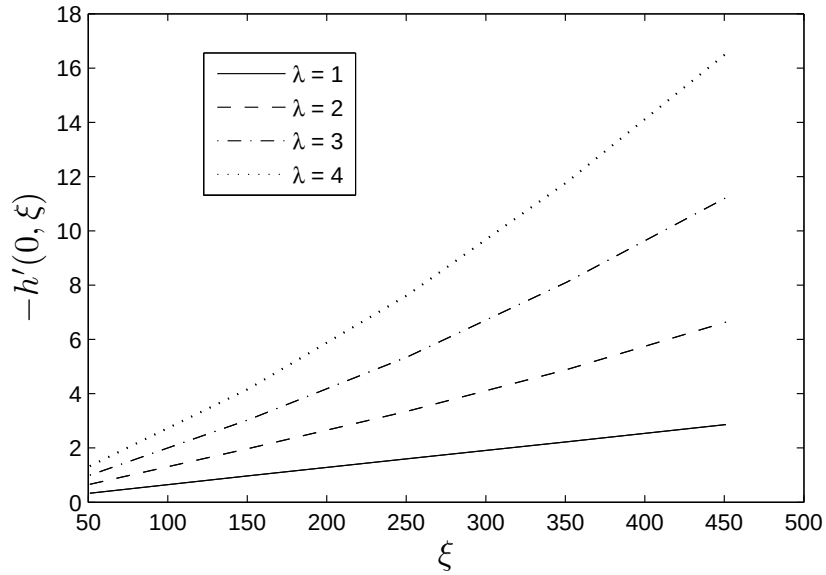

Figure 5.5: Skin friction variation for different values of λ

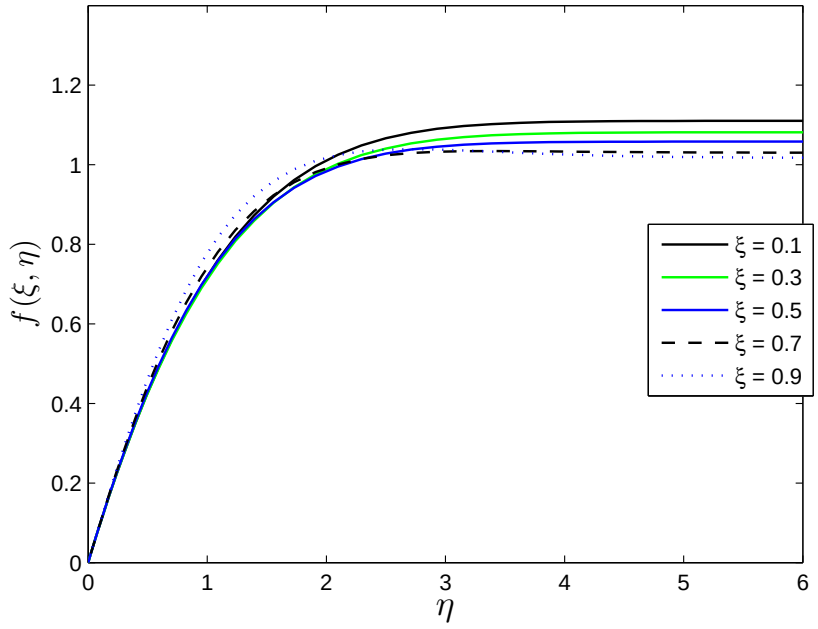

Figure 5.6: velocity profile for different value of ξ

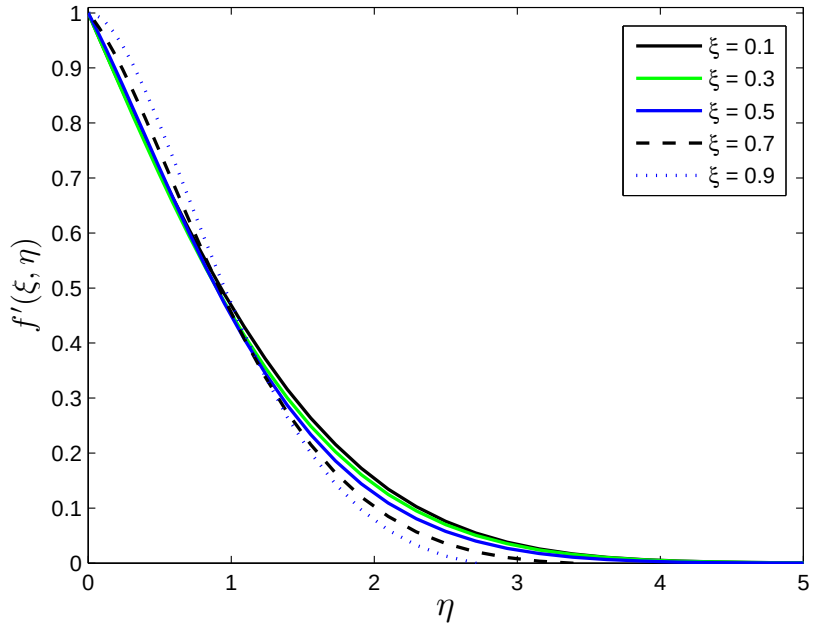

Figure 5.7: Velocity profiles for different values of ξ when $\lambda = 1$

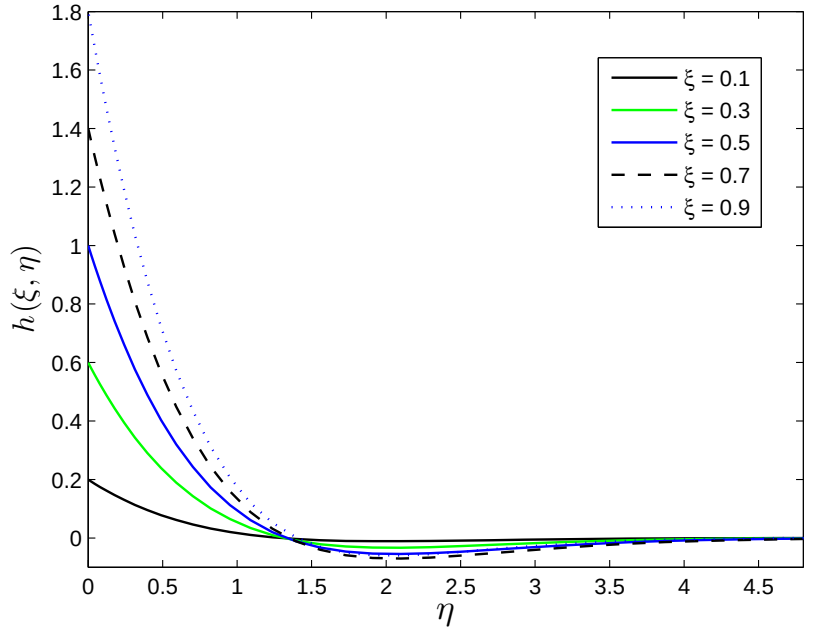

Figure 5.8: Velocity profiles for different values of ξ when $\lambda = 1$

Conclusion

In this thesis, we considered the spectral local linearisation method approach for solving an coupled non-linear partial differential equation system that governs two-dimensional an incompressible rotating viscous fluid flow due to unsteady stretching surface. A considerable advantage was found with the use of a transformed, finite time scale in which $\tau = \infty$ corresponds to $\xi = 1$, when the governing equation can be solved by means of smooth transition from the small time solution to the large time solution. The effect of the physical parameters λ on the flow characteristics as well as the axial and angular skin friction coefficients have been studied graphically and in tabular form. The most important finding is that the transition from the initial unsteady state flow to the final steady state flow takes place smoothly and without any singularity.

References

[1] B.C. Sakiadis, Boundary layer behaviour on continuous solid surface: I. Boundary layer equations for two-dimensional and axismmetric flow. *AIChE Journal* 7 (1961) 26-28.

[2] B.C. Sakiadis, Boundary layer behaviour on continuous solid surface: II. Boundary layer equations for two-dimensional and axismmetric flow, *AIChE Journal*. 7 (1961) 221-225.

[3] L. Crane, Flow past a stretching plate, *Z Angew Math Phys*, 21 (1970) 645-647.

[4] J.F. Brady and A. Acrivos, Steady flow in a channel or tube with an accelerating surface velocity. J. Fluid Mech. 112 (1981) 127-150.

[5] C.Y. Wang, The three-dimensional flow due to a stretching flat surface. *Phys. Fluids*, 27 (1984) 1915-1917.

[6] N. Afzal, Heat transfer froma stretching surface, *International Journal of Heat and Mass Transfer*, 36 (1993) 1128-1131.

[7] K.V. Prasad, S. Abel, P.S. Datti Diffusion of chemically reactive species of a non-Newtonian fluid immersed in a porous medium over a stretching sheet *International Journal of Non- Linear Mechanics*, 38 (2003) 651-657.

[8] M.S. Abel and N. Mahesha, Heat transfer in MHD viscoelastic fluid flow over a stretching sheet with variable thermal conductivity, non-uniform heat source and radiation, *Applied Mathematical Modelling*, 32 (2008) 1965-1983.

[9] M.S. Abel,P.G. Siddheshwar and M.M. Nandeppanavar, Heat transfer in a viscoelastic boundary layer flow over a stretching sheet with viscous dissipation and non-uniform heat source. *International Journal of Heat andMass Transfer*, 50 (2007) 960-966.

[10] R.C. Bataller, Viscoelastic fluid flow and heat transfer over a stretching sheet under the effects of a non-uniform heat source, viscous dissipation and thermal radiation, *International Journal of Heat and Mass Transfer*, 50 (2007) 315-31620.

[11] V.M. Soundalgekar, B.W. Martin, S.K. Gupta and I. Pop, On Unsteady Boundary Layer in a Rotating Fluid with Time dependant suction, *Publication De LInstitute Mathematique*, 20 (1976) 215-226. 12.

[12] R.W. Bergstrom, Viscous Boundary Layers in Rotating Fluids Driven by Periodic Flows, *J. Atmos. Sci*, 33(1976) 1234-1247.

[13] Z. Abbas, T. Javed, M. Sajid and N. Ali, Unsteady MHD flow and heat transfer on a stretching sheet in a rotating fluid, *Journal of the Taiwan Institute of Chemical Engineers*, 41 (2010) 644-650.

[14] R. Nazar, N. Amin and I. Pop, Unsteady boundary layer flow due to a stretching surface in a rotating fluid, *Mechanics Research Communications*, 31 (2004) 121-128.

[15] L. Zheng,C. Li, X. Zhang and Y. Gao, Exact solutions for the unsteady rotating flows of a generalized Maxwell fluid with oscil-

lating pressure gradient between coaxial cylinders, *Computers & Mathematics with Applications*, 62(2011) 1105-1115.

[16] T. Fang and H. Tao, Unsteady viscous flow over a rotating stretchable disk with deceleration, *Communications in Nonlinear Science and Numerical Simulation*, 17 (2012) 5064-5072.

[17] A. M. Rashad, Effects of radiation and variable viscosity on unsteady MHD flow of a rotating fluid from stretching surface in porous media, *Journal of the Egyptian Mathematical Society*, 22 (2014) 134-142.

[18] Najeeb.A. Khan, S. Aziz and Nadeem.A. Khan, Numerical simulation for the unsteady MHD flow and heat transfer of couple stress fluid over a rotating disk, *PLoS ONE*, 9 (2014) e95423. doi:10.1371/journal.pone.0095423. 19.

[19] M.R Hajmohammadi, S.S. Nourazar and A. Campo, Analytical solution for two-phase flow betwen two rotating cylinders filed with power law liquid and a micro layer of gas, *Journal of Mechanical Science and Technology* 28 (2014) 1849-1854.

[20] M.R Hajmohammadi S.S. Nourazar, On the insertion of a thin gas layer in micro cylindrical Couette flows involving power-law liquids, *International Journal of Heat and Mass Transfer*, 75 (2014) 97-108.

[21] S. S. Motsa, P. G. Dlamini and M. Khumalo, Spectral Relaxation Method and Spectral Quasilinearization Method for Solving Unsteady Boundary Layer Flow Problems, *Advances in Mathematical Physics*, Vol 2014 (2014), Article ID 341964, 12 pages http://dx.doi.org/10.1155/2014/341964.

[22] S. S. Motsa and Z. G. Makukula, On spectral relaxation method approach for steady von Krmn flow of a Reiner-Rivlin fluid with

Joule heating, viscous dissipation and suction/injection, *Central European Journal of Physics*, 11 (2013) 363-374, 2013.

[23] S. Motsa, P. Dlamini, and M. Khumalo, A new multistage spectral relaxation method for solving chaotic initial value systems, *Nonlinear Dynamics*, 72 (2013) 265-283.

[24] S. S. Motsa, P. G. Dlamini, and M. Khumalo, Solving hyperchaotic systems using the spectral relaxation method, *Abstract and Applied Analysis*, Vol 2012, Article ID 203461, 18 pages.

[25] R. Nazar, N. Amin I. Pop, Unsteady boundary layer flow due to a stretching surface in a rorating fluid, *Mechanics Research Conmmunications*, 31 (2004) 121 - 128.

[26] T. Cebeci and P. Bradshaw, Physical and Computational Aspects of Convective Heat Transfer, *Springer, New York*, NY, USA, 1984.